

$\mu \rightarrow e\gamma$ Decay in an MSSM ExtensionTarek Ibrahim^{a*}, Ahmad Itani^b and Pran Nath^{c†}

a. University of Science and Technology, Zewail City of Science and Technology,
6th of October City, Giza 12588, Egypt³

b. Department of Physics, Faculty of Science, Beirut Arab University, Beirut, Lebanon⁴

c. Department of Physics, Northeastern University, Boston, MA 02115-5000, USA

Abstract

An analysis is given of the decay $\mu \rightarrow e + \gamma$ in an MSSM extension with a vectorlike generation. Here mixing with the mirrors allows the possibility of this decay. The analysis is done at the one loop level with the exchange of charginos and neutralinos and of sleptons and mirror sleptons in the loops. A one loop analysis with W and Z boson exchange and mirror leptons and neutrinos is also considered. The effects of CP violating phases from the new sector on the decay $\mu \rightarrow e\gamma$ are analyzed in detail. The constraints arising from the current upper limit on the branching ratio $\mathcal{B}(\mu \rightarrow e\gamma)$ from the MEG experiment of 2.4×10^{-12} (at 90% CL) on the parameter space of SUSY models and on vectorlike models are explored. Further, the MEG experiment is likely to improve the upper limit by an order of magnitude in the coming years. The improved limits will allow one to probe a much larger domain of the parameter space of the extended models.

Keywords: Lepton flavor change, $\mu \rightarrow e\gamma$, vector multiplets, MSSM extension.

PACS numbers: 13.40Em, 12.60.-i, 14.60.Fg

*Email: tbrahim@zewailcity.edu.eg

†Email: nath@neu.edu

³Permanent address: Department of Physics, Faculty of Science, University of Alexandria, Alexandria, Egypt

⁴Email: a.itanis@bau.edu.lb

1 Introduction

Lepton flavor violation provides a new window for physics beyond the standard model. Since there is no CKM type matrix in the charged leptonic sector, flavor violations involving charged leptons arise via loop corrections which in particular can produce charged lepton flavor violating processes such as $\ell_i^\pm \rightarrow \ell_j^\pm \gamma$. Recently the MEG experiment [1] has put the most stringent bound thus far on the lepton flavor violating decay $\mu \rightarrow e \gamma$ so that

$$\mathcal{B}(\mu \rightarrow e + \gamma) < 2.4 \times 10^{-12} \quad \text{at 90\% CL (MEG)}. \quad (1)$$

In this work we explore the implications of a new leptonic vector generation for the $\mu \rightarrow e + \gamma$ decay. Specifically we consider an additional generation of leptons and their mirrors that mix with the three ordinary generations of leptons. Inclusion of a vectorlike generation brings in new sources of CP violation which enter in $\mu \rightarrow e \gamma$ decay. These arise from diagrams where one has charginos and sneutrinos and neutralinos and charged sleptons in the loops. Additionally one has diagrams with W and neutrinos and Z and charged leptons in the loops. Such diagrams can produce observable effects and thus the experimental upper limit constrains the parameter space of models. Specifically we will show that the $\mu \rightarrow e \gamma$ process can allow one to probe new physics arising from the MSSM extension. The reason for considering a vectorlike leptonic generation is the following: First vectorlike generations naturally appear in a variety of grand unified models, string models and D brane models and some of these can survive down to low scales[2]. Second a vectorlike generation is anomaly free so the good properties of the model as a quantum field theory are protected. In previous works [3, 4, 5, 6, 7, 8, 9, 10, 11, 12, 13] we have considered the effects of an extra vectorlike generation on a number of processes and here we extend the analysis to discuss $\mu \rightarrow e \gamma$ decay which is one of most stringently constrained lepton flavor violating process. We also investigate the effect of CP phases on the decay $\mu \rightarrow e \gamma$. Vectorlike multiplets have also been used by other authors (see, e.g., [14, 15, 16]). Further, $\mu \rightarrow e \gamma$ decay has been analyzed in several previous works (see, e.g., [17, 18, 19, 20, 21, 22, 23]). However, none of the previous works explore the class of models discussed here.

The outline of the rest of the paper is as follows: In section 2 we define the model with an extra vectorlike leptonic generation and specify the nature of mixings between the extra vectorlike generation and the three ordinary generations. In section 3 we give the interactions of the leptons and mirror leptons with the charginos and the neutralinos in the mass diagonal basis. In section 4 we give an analysis of the interactions of the leptons and their mirrors with the W and Z bosons. An analytic analysis of $\mu \rightarrow e \gamma$ decay is given in section 5 which includes charginos and neutralinos in the loops as well as W and Z bosons in the loops. A numerical analysis of the $\mu \rightarrow e \gamma$ branching ratio is given in section 6. Here it is shown that the vectorlike

generation gives a significantly large contribution which allows one to probe and constrain the extended model. It is known that CP phases can have a large effect on SUSY loop corrections (for a review see [24]) and thus the effect of CP phases on the decay $\mu \rightarrow e\gamma$ is also analyzed. Conclusions are given in section 7. Details of the scalar mass squared matrices are given in section 8.

2 Extension of MSSM with a Vector Multiplet

In this section we extend MSSM to include a vectorlike generation which consists of an ordinary fourth generation of leptons, quarks and their mirrors. As mentioned in section 1 vectorlike multiplets arise in a variety of unified models some of which could be low lying. In the analysis below we will assume an extended MSSM with just one vector multiplet. Before proceeding further we define the notation and give a very brief description of the extended model and a more detailed description can be found in the previous works mentioned above. Thus the extended MSSM contains a vectorlike multiplet. To fix notation the three generations of leptons are denoted by

$$\psi_{iL} \equiv \begin{pmatrix} \nu_{iL} \\ l_{iL} \end{pmatrix} \sim (1, 2, -\frac{1}{2}); \quad l_{iL}^c \sim (1, 1, 1); \quad \nu_{iL}^c \sim (1, 1, 0); \quad i = 1, 2, 3 \quad (2)$$

where the properties under $SU(3)_C \times SU(2)_L \times U(1)_Y$ are also exhibited. The last entry in the braces such as $(1, 2, -1/2)$ is the value of the hypercharge Y defined so that $Q = T_3 + Y$. These leptons have $V - A$ interactions. We can now add a vectorlike multiplet where we have a fourth family of leptons with $V - A$ interactions whose transformations can be gotten from Eq.(2) by letting i run from 1 to 4. A vectorlike lepton multiplet also has mirrors and so we consider these mirror leptons which have $V + A$ interactions. The quantum numbers of the mirrors are given by

$$\chi^c \equiv \begin{pmatrix} E_L^c \\ N_L^c \end{pmatrix} \sim (1, 2, \frac{1}{2}); \quad E_L \sim (1, 1, -1); \quad N_L \sim (1, 1, 0). \quad (3)$$

Interesting new physics arises when we allow mixings of the vectorlike generation with the three ordinary generations. Here we focus on the mixing of the mirrors in the vectorlike generation with the three generations. Thus the superpotential of the model allowing for the mixings among the three ordinary generations and the vectorlike generation is given by

$$\begin{aligned}
W = & -\mu\epsilon_{ij}\hat{H}_1^i\hat{H}_2^j + \epsilon_{ij}[f_1\hat{H}_1^i\hat{\psi}_L^j\hat{\tau}_L^c + f'_1\hat{H}_2^j\hat{\psi}_L^i\hat{\nu}_{\tau L}^c + f_2\hat{H}_1^i\hat{\chi}^{cj}\hat{N}_L + f'_2\hat{H}_2^j\hat{\chi}^{ci}\hat{E}_L \\
& + h_1H_1^i\hat{\psi}_{\mu L}^j\hat{\mu}_L^c + h'_1H_2^j\hat{\psi}_{\mu L}^i\hat{\nu}_{\mu L}^c + h_2H_1^i\hat{\psi}_{eL}^j\hat{e}_L^c + h'_2H_2^j\hat{\psi}_{eL}^i\hat{\nu}_{eL}^c] \\
& + f_3\epsilon_{ij}\hat{\chi}^{ci}\hat{\psi}_L^j + f'_3\epsilon_{ij}\hat{\chi}^{ci}\hat{\psi}_{\mu L}^j + f_4\hat{\tau}_L^c\hat{E}_L + f_5\hat{\nu}_{\tau L}^c\hat{N}_L + f'_4\hat{\mu}_L^c\hat{E}_L + f'_5\hat{\nu}_{\mu L}^c\hat{N}_L \\
& + f''_3\epsilon_{ij}\hat{\chi}^{ci}\hat{\psi}_{eL}^j + f''_4\hat{e}_L^c\hat{E}_L + f''_5\hat{\nu}_{eL}^c\hat{N}_L, \tag{4}
\end{aligned}$$

where $\hat{}$ implies superfields, $\hat{\psi}_L$ stands for $\hat{\psi}_{3L}$, $\hat{\psi}_{\mu L}$ stands for $\hat{\psi}_{2L}$ and $\hat{\psi}_{eL}$ stands for $\hat{\psi}_{1L}$. In eq. (4) we have suppressed terms such as $e_4^c E_L$ etc for simplicity. Their inclusion will not change our analysis substantially.

The mass terms for the neutrinos, mirror neutrinos, leptons and mirror leptons arise from the term

$$\mathcal{L} = -\frac{1}{2}\frac{\partial^2 W}{\partial A_i \partial A_j}\psi_i\psi_j + \text{H.c.}, \tag{5}$$

where ψ and A stand for generic two-component fermion and scalar fields. After spontaneous breaking of the electroweak symmetry, ($\langle H_1^1 \rangle = v_1/\sqrt{2}$ and $\langle H_2^2 \rangle = v_2/\sqrt{2}$), we have the following set of mass terms written in the 4-component spinor notation so that

$$-\mathcal{L}_m = \bar{\xi}_R^T(M_f)\xi_L + \bar{\eta}_R^T(M_\ell)\eta_L + \text{H.c.}, \tag{6}$$

where the basis vectors in which the mass matrix is written is given by

$$\begin{aligned}
\bar{\xi}_R^T &= (\bar{\nu}_{\tau R} \quad \bar{N}_R \quad \bar{\nu}_{\mu R} \quad \bar{\nu}_{eR}), \\
\xi_L^T &= (\nu_{\tau L} \quad N_L \quad \nu_{\mu L} \quad \nu_{eL}), \\
\bar{\eta}_R^T &= (\bar{\tau}_R \quad \bar{E}_R \quad \bar{\mu}_R \quad \bar{e}_R), \\
\eta_L^T &= (\tau_L \quad E_L \quad \mu_L \quad e_L), \tag{7}
\end{aligned}$$

and the mass matrix M_f is given by

$$M_f = \begin{pmatrix} f'_1 v_2/\sqrt{2} & f_5 & 0 & 0 \\ -f_3 & f_2 v_1/\sqrt{2} & -f'_3 & -f''_3 \\ 0 & f'_5 & h'_1 v_2/\sqrt{2} & 0 \\ 0 & f''_5 & 0 & h'_2 v_2/\sqrt{2} \end{pmatrix}. \tag{8}$$

We define the matrix element (22) of the mass matrix as m_N so that

$$m_N = f_2 v_1/\sqrt{2}. \tag{9}$$

The mass matrix is not hermitian and thus one needs bi-unitary transformations to diagonalize it. We define the bi-unitary transformation so that

$$D_R^{\nu\dagger}(M_f)D_L^\nu = \text{diag}(m_{\psi_1}, m_{\psi_2}, m_{\psi_3}, m_{\psi_4}). \quad (10)$$

Under the bi-unitary transformations the basis vectors transform so that

$$\begin{pmatrix} \nu_{\tau R} \\ \tilde{N}_R \\ \nu_{\mu R} \\ \nu_{e R} \end{pmatrix} = D_R^\nu \begin{pmatrix} \psi_{1R} \\ \psi_{2R} \\ \psi_{3R} \\ \psi_{4R} \end{pmatrix}, \quad \begin{pmatrix} \nu_{\tau L} \\ \tilde{N}_L \\ \nu_{\mu L} \\ \nu_{e L} \end{pmatrix} = D_L^\nu \begin{pmatrix} \psi_{1L} \\ \psi_{2L} \\ \psi_{3L} \\ \psi_{4L} \end{pmatrix}. \quad (11)$$

In $\psi_1, \psi_2, \psi_3, \psi_4$ are the mass eigenstates for the neutrinos, where in the limit of no mixing we identify ψ_1 as the light tau neutrino, ψ_2 as the heavier mass eigenstate, ψ_3 as the muon neutrino and ψ_4 as the electron neutrino. A similar analysis goes to the lepton mass matrix M_ℓ where

$$M_\ell = \begin{pmatrix} f_1 v_1/\sqrt{2} & f_4 & 0 & 0 \\ f_3 & f'_2 v_2/\sqrt{2} & f'_3 & f''_3 \\ 0 & f'_4 & h_1 v_1/\sqrt{2} & 0 \\ 0 & f''_4 & 0 & h_2 v_1/\sqrt{2} \end{pmatrix}. \quad (12)$$

In general $f_3, f_4, f_5, f'_3, f'_4, f'_5, f''_3, f''_4, f''_5$ can be complex and we define their phases so that

$$f_k = |f_k|e^{i\chi_k}, \quad f'_k = |f'_k|e^{i\chi'_k}, \quad f''_k = |f''_k|e^{i\chi''_k}; k = 3, 4, 5. \quad (13)$$

We introduce now the mass parameter m_E defined by the (22) element of the mass matrix above so that

$$m_E = f'_2 v_2/\sqrt{2}. \quad (14)$$

Next we consider the mixing of the charged sleptons and the charged mirror sleptons. The mass squared matrix of the slepton - mirror slepton comes from three sources: the F term, the D term of the potential and the soft SUSY breaking terms. Using the superpotential of Eq. (4), the mass terms arising from it after the breaking of the electroweak symmetry are given by the Lagrangian

$$\mathcal{L} = \mathcal{L}_F + \mathcal{L}_D + \mathcal{L}_{\text{soft}}, \quad (15)$$

where \mathcal{L}_F is deduced from $F_i = \partial W/\partial A_i$, and $-\mathcal{L}_F = V_F = F_i F_i^*$ is given in the appendix, while the \mathcal{L}_D is given by

$$\begin{aligned} -\mathcal{L}_D = & \frac{1}{2}m_Z^2 \cos^2 \theta_W \cos 2\beta \{ \tilde{\nu}_{\tau L} \tilde{\nu}_{\tau L}^* - \tilde{\tau}_L \tilde{\tau}_L^* + \tilde{\nu}_{\mu L} \tilde{\nu}_{\mu L}^* - \tilde{\mu}_L \tilde{\mu}_L^* + \tilde{\nu}_{e L} \tilde{\nu}_{e L}^* - \tilde{e}_L \tilde{e}_L^* \\ & + \tilde{E}_R \tilde{E}_R^* - \tilde{N}_R \tilde{N}_R^* \} + \frac{1}{2}m_Z^2 \sin^2 \theta_W \cos 2\beta \{ \tilde{\nu}_{\tau L} \tilde{\nu}_{\tau L}^* + \tilde{\tau}_L \tilde{\tau}_L^* + \tilde{\nu}_{\mu L} \tilde{\nu}_{\mu L}^* + \tilde{\mu}_L \tilde{\mu}_L^* \\ & + \tilde{\nu}_{e L} \tilde{\nu}_{e L}^* + \tilde{e}_L \tilde{e}_L^* - \tilde{E}_R \tilde{E}_R^* - \tilde{N}_R \tilde{N}_R^* + 2\tilde{E}_L \tilde{E}_L^* - 2\tilde{\tau}_R \tilde{\tau}_R^* - 2\tilde{\mu}_R \tilde{\mu}_R^* - 2\tilde{e}_R \tilde{e}_R^* \}. \end{aligned} \quad (16)$$

For $\mathcal{L}_{\text{soft}}$ we assume the following form

$$\begin{aligned}
-\mathcal{L}_{\text{soft}} = & M_{\tilde{\tau}_L}^2 \tilde{\psi}_{\tau L}^{i*} \tilde{\psi}_{\tau L}^i + M_{\tilde{\chi}}^2 \tilde{\chi}^{ci*} \tilde{\chi}^{ci} + M_{\tilde{\mu}_L}^2 \tilde{\psi}_{\mu L}^{i*} \tilde{\psi}_{\mu L}^i + M_{\tilde{e}_L}^2 \tilde{\psi}_{eL}^{i*} \tilde{\psi}_{eL}^i + M_{\tilde{\nu}_\tau}^2 \tilde{\nu}_{\tau L}^{c*} \tilde{\nu}_{\tau L}^c + M_{\tilde{\nu}_\mu}^2 \tilde{\nu}_{\mu L}^{c*} \tilde{\nu}_{\mu L}^c \\
& + M_{\tilde{\nu}_e}^2 \tilde{\nu}_{eL}^{c*} \tilde{\nu}_{eL}^c + M_{\tilde{\tau}}^2 \tilde{\tau}_L^{c*} \tilde{\tau}_L^c + M_{\tilde{\mu}}^2 \tilde{\mu}_L^{c*} \tilde{\mu}_L^c + M_{\tilde{e}}^2 \tilde{e}_L^{c*} \tilde{e}_L^c + M_{\tilde{E}}^2 \tilde{E}_L^* \tilde{E}_L + M_{\tilde{N}}^2 \tilde{N}_L^* \tilde{N}_L \\
& + \epsilon_{ij} \{ f_1 A_\tau H_1^i \tilde{\psi}_{\tau L}^j \tilde{\tau}_L^c - f'_1 A_{\nu_\tau} H_2^i \tilde{\psi}_{\tau L}^j \tilde{\nu}_{\tau L}^c + h_1 A_\mu H_1^i \tilde{\psi}_{\mu L}^j \tilde{\mu}_L^c - h'_1 A_{\nu_\mu} H_2^i \tilde{\psi}_{\mu L}^j \tilde{\nu}_{\mu L}^c \\
& + h_2 A_e H_1^i \tilde{\psi}_{eL}^j \tilde{e}_L^c - h'_2 A_{\nu_e} H_2^i \tilde{\psi}_{eL}^j \tilde{\nu}_{eL}^c + f_2 A_N H_1^i \tilde{\chi}^{cj} \tilde{N}_L - f'_2 A_E H_2^i \tilde{\chi}^{cj} \tilde{E}_L + \text{H.c.} \} . \tag{17}
\end{aligned}$$

Here $M_{\tilde{e}_L}, M_{\tilde{\nu}_e}$ etc are the soft masses and A_e, A_{ν_e} etc are the trilinear couplings. The trilinear couplings are complex and we define their phases so that

$$A_e = |A_e| e^{i\alpha_{A_e}} , \quad A_{\nu_e} = |A_{\nu_e}| e^{i\alpha_{A_{\nu_e}}} , \dots . \tag{18}$$

From these terms we construct the scalar mass square matrices. These are exhibited in section 8.

3 Interactions with charginos and neutralinos

In this section we discuss the interactions in the mass diagonal basis involving charged leptons, sneutrinos and charginos. Thus we have

$$-\mathcal{L}_{\tau-\tilde{\nu}-\chi^-} = \sum_{i=1}^2 \sum_{j=1}^8 \tilde{\tau}_\alpha (C_{\alpha ij}^L P_L + C_{\alpha ij}^R P_R) \tilde{\chi}^{ci} \tilde{\nu}_j + \text{H.c.}, \tag{19}$$

such that

$$\begin{aligned}
C_{\alpha ij}^L = & g(-\kappa_\tau U_{i2}^* D_{R1\alpha}^{\tau*} \tilde{D}_{1j}^\nu - \kappa_\mu U_{i2}^* D_{R3\alpha}^{\tau*} \tilde{D}_{5j}^\nu - \kappa_e U_{i2}^* D_{R4\alpha}^{\tau*} \tilde{D}_{7j}^\nu \\
& + U_{i1}^* D_{R2\alpha}^{\tau*} \tilde{D}_{4j}^\nu - \kappa_N U_{i2}^* D_{R2\alpha}^{\tau*} \tilde{D}_{2j}^\nu) \tag{20}
\end{aligned}$$

$$\begin{aligned}
C_{\alpha ij}^R = & g(-\kappa_{\nu_\tau} V_{i2} D_{L1\alpha}^{\tau*} \tilde{D}_{3j}^\nu - \kappa_{\nu_\mu} V_{i2} D_{L3\alpha}^{\tau*} \tilde{D}_{6j}^\nu - \kappa_{\nu_e} V_{i2} D_{L4\alpha}^{\tau*} \tilde{D}_{8j}^\nu + V_{i1} D_{L1\alpha}^{\tau*} \tilde{D}_{1j}^\nu \\
& + V_{i1} D_{L3\alpha}^{\tau*} \tilde{D}_{5j}^\nu + V_{i1} D_{L4\alpha}^{\tau*} \tilde{D}_{7j}^\nu - \kappa_E V_{i2} D_{L2\alpha}^{\tau*} \tilde{D}_{4j}^\nu), \tag{21}
\end{aligned}$$

with

$$(\kappa_N, \kappa_\tau, \kappa_\mu, \kappa_e) = \frac{(m_N, m_\tau, m_\mu, m_e)}{\sqrt{2} m_W \cos \beta}, \tag{22}$$

$$(\kappa_E, \kappa_{\nu_\tau}, \kappa_{\nu_\mu}, \kappa_{\nu_e}) = \frac{(m_E, m_{\nu_\tau}, m_{\nu_\mu}, m_{\nu_e})}{\sqrt{2} m_W \sin \beta}. \tag{23}$$

and

$$U^* M_C V = \text{diag}(m_{\tilde{\chi}_1^-}, m_{\tilde{\chi}_2^-}). \quad (24)$$

Next we discuss the interactions in the mass diagonal basis involving charged leptons, sleptons and neutralinos. Thus we have

$$-\mathcal{L}_{\tau-\tilde{\tau}-\chi^0} = \sum_{i=1}^4 \sum_{j=1}^8 \bar{\tau}_\alpha (C'_{\alpha ij}{}^L P_L + C'_{\alpha ij}{}^R P_R) \tilde{\chi}_i^0 \tilde{\tau}_j + \text{H.c.}, \quad (25)$$

such that

$$\begin{aligned} C'_{\alpha ij}{}^L = & \sqrt{2}(\alpha_{\tau i} D_{R1\alpha}^{\tau*} \tilde{D}_{1j}^\tau - \delta_{Ei} D_{R2\alpha}^{\tau*} \tilde{D}_{2j}^\tau - \gamma_{\tau i} D_{R1\alpha}^{\tau*} \tilde{D}_{3j}^\tau + \beta_{Ei} D_{R2\alpha}^{\tau*} \tilde{D}_{4j}^\tau + \alpha_{\mu i} D_{R3\alpha}^{\tau*} \tilde{D}_{5j}^\tau \\ & - \gamma_{\mu i} D_{R3\alpha}^{\tau*} \tilde{D}_{6j}^\tau + \alpha_{ei} D_{R4\alpha}^{\tau*} \tilde{D}_{7j}^\tau - \gamma_{ei} D_{R4\alpha}^{\tau*} \tilde{D}_{8j}^\tau) \end{aligned} \quad (26)$$

$$\begin{aligned} C'_{\alpha ij}{}^R = & \sqrt{2}(\beta_{\tau i} D_{L1\alpha}^{\tau*} \tilde{D}_{1j}^\tau - \gamma_{Ei} D_{L2\alpha}^{\tau*} \tilde{D}_{2j}^\tau - \delta_{\tau i} D_{L1\alpha}^{\tau*} \tilde{D}_{3j}^\tau + \alpha_{Ei} D_{L2\alpha}^{\tau*} \tilde{D}_{4j}^\tau + \beta_{\mu i} D_{L3\alpha}^{\tau*} \tilde{D}_{5j}^\tau \\ & - \delta_{\mu i} D_{L3\alpha}^{\tau*} \tilde{D}_{6j}^\tau + \beta_{ei} D_{L4\alpha}^{\tau*} \tilde{D}_{7j}^\tau - \delta_{ei} D_{L4\alpha}^{\tau*} \tilde{D}_{8j}^\tau), \end{aligned} \quad (27)$$

where

$$\alpha_{Ei} = \frac{gm_E X_{4i}^*}{2m_W \sin \beta}, \quad \beta_{Ei} = eX'_{1i} + \frac{g}{\cos \theta_W} X'_{2i} \left(\frac{1}{2} - \sin^2 \theta_W \right), \quad (28)$$

$$\gamma_{Ei} = eX'_{1i} - \frac{g \sin^2 \theta_W}{\cos \theta_W} X'_{2i}, \quad \delta_{Ei} = -\frac{gm_E X_{4i}}{2m_W \sin \beta}, \quad (29)$$

and

$$\alpha_{\tau i} = \frac{gm_\tau X_{3i}}{2m_W \cos \beta}, \quad \alpha_{\mu i} = \frac{gm_\mu X_{3i}}{2m_W \cos \beta}, \quad \alpha_{ei} = \frac{gm_e X_{3i}}{2m_W \cos \beta}, \quad (30)$$

$$\delta_{\tau i} = -\frac{gm_\tau X_{3i}^*}{2m_W \cos \beta}, \quad \delta_{\mu i} = -\frac{gm_\mu X_{3i}^*}{2m_W \cos \beta}, \quad \delta_{ei} = -\frac{gm_e X_{3i}^*}{2m_W \cos \beta}, \quad (31)$$

and where

$$\beta_{\tau i} = \beta_{\mu i} = \beta_{ei} = -eX'_{1i} + \frac{g}{\cos \theta_W} X'_{2i} \left(-\frac{1}{2} + \sin^2 \theta_W \right), \quad (32)$$

$$\gamma_{\tau i} = \gamma_{\mu i} = \gamma_{ei} = -eX'_{1i} + \frac{g \sin^2 \theta_W}{\cos \theta_W} X'_{2i}. \quad (33)$$

Here X' are defined by

$$X'_{1i} = X_{1i} \cos \theta_W + X_{2i} \sin \theta_W, \quad (34)$$

$$X'_{2i} = -X_{1i} \sin \theta_W + X_{2i} \cos \theta_W, \quad (35)$$

where X diagonalizes the neutralino mass matrix and is defined by the relation

$$X^T M_{\tilde{\chi}^0} X = \text{diag}(m_{\chi_1^0}, m_{\chi_2^0}, m_{\chi_3^0}, m_{\chi_4^0}). \quad (36)$$

4 Interaction of leptons and mirrors with W and Z bosons

In addition to the computation of the supersymmetric loop diagrams, we compute the contributions arising from the exchange of the W and Z bosons and the leptons and the mirror leptons in the loops. The relevant interactions needed are given below. For the W boson exchange the interactions that enter are given by

$$-\mathcal{L}_{\tau W \psi} = W_\rho^\dagger \sum_{i=1}^4 \sum_{\alpha=1}^4 \bar{\psi}_i \gamma^\rho [C_{L_{i\alpha}}^W P_L + C_{R_{i\alpha}}^W P_R] \tau_\alpha + \text{H.c.}, \quad (37)$$

where

$$C_{L_{i\alpha}}^W = \frac{g}{\sqrt{2}} [D_{L_{1i}}^{\nu*} D_{L_{1\alpha}}^\tau + D_{L_{3i}}^{\nu*} D_{L_{3\alpha}}^\tau + D_{L_{4i}}^{\nu*} D_{L_{4\alpha}}^\tau], \quad (38)$$

$$C_{R_{i\alpha}}^W = \frac{g}{\sqrt{2}} [D_{R_{2i}}^{\nu*} D_{R_{2\alpha}}^\tau]. \quad (39)$$

For the Z boson exchange the interactions that enter are given by

$$-\mathcal{L}_{\tau\tau Z} = Z_\rho \sum_{\alpha=1}^4 \sum_{\beta=1}^4 \bar{\tau}_\alpha \gamma^\rho [C_{L_{\alpha\beta}}^Z P_L + C_{R_{\alpha\beta}}^Z P_R] \tau_\beta, \quad (40)$$

where

$$C_{L_{\alpha\beta}}^Z = \frac{g}{\cos \theta_W} [x(D_{L_{\alpha 1}}^{\tau\dagger} D_{L_{1\beta}}^\tau + D_{L_{\alpha 2}}^{\tau\dagger} D_{L_{2\beta}}^\tau + D_{L_{\alpha 3}}^{\tau\dagger} D_{L_{3\beta}}^\tau + D_{L_{\alpha 4}}^{\tau\dagger} D_{L_{4\beta}}^\tau) - \frac{1}{2}(D_{L_{\alpha 1}}^{\tau\dagger} D_{L_{1\beta}}^\tau + D_{L_{\alpha 3}}^{\tau\dagger} D_{L_{3\beta}}^\tau + D_{L_{\alpha 4}}^{\tau\dagger} D_{L_{4\beta}}^\tau)], \quad (41)$$

and

$$C_{R_{\alpha\beta}}^Z = \frac{g}{\cos \theta_W} [x(D_{R_{\alpha 1}}^{\tau\dagger} D_{R_{1\beta}}^\tau + D_{R_{\alpha 2}}^{\tau\dagger} D_{R_{2\beta}}^\tau + D_{R_{\alpha 3}}^{\tau\dagger} D_{R_{3\beta}}^\tau + D_{R_{\alpha 4}}^{\tau\dagger} D_{R_{4\beta}}^\tau) - \frac{1}{2}(D_{R_{\alpha 2}}^{\tau\dagger} D_{R_{2\beta}}^\tau)], \quad (42)$$

where $x = \sin^2 \theta_W$.

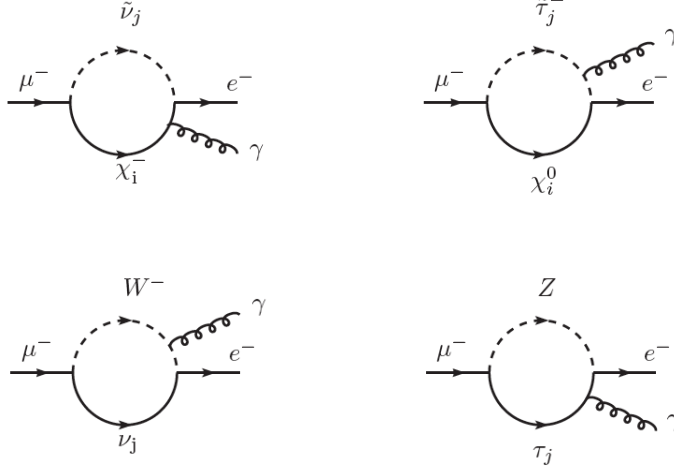


Figure 1: The diagrams that allow the decay of $\mu \rightarrow e + \gamma$ via supersymmetric loops involving the chargino (top left) and the neutralino (top right) and via W loop (bottom left) and Z loop (bottom right) with emission of the photon from the charged particle inside the loop.

5 The analysis of $\mu \rightarrow e + \gamma$ Branching Ratio

The decay $\mu \rightarrow e + \gamma$ is induced by one-loop electric and magnetic transition dipole moments, which arise from the diagrams of Fig.5. For an incoming muon of momentum p and a resulting electron of momentum p' , we define the amplitude

$$\langle e(p') | J_\alpha | \mu(p) \rangle = \bar{u}_e(p') \Gamma_\alpha u_\mu(p), \quad (43)$$

where

$$\Gamma_\alpha(q) = \frac{F_2^{\mu e}(q) i \sigma_{\alpha\beta} q^\beta}{m_\mu + m_e} + \frac{F_3^{\mu e}(q) \sigma_{\alpha\beta} \gamma_5 q^\beta}{m_\mu + m_e} + \dots \quad (44)$$

with $q = p' - p$ and where m_f denotes the mass of the fermion f . The branching ratio of $\mu \rightarrow e + \gamma$ is given by

$$\mathcal{B}(\mu \rightarrow e + \gamma) = \frac{24\pi^2}{G_F^2 m_\mu^2 (m_\mu + m_e)^2} \{ |F_2^{\mu e}(0)|^2 + |F_3^{\mu e}(0)|^2 \}, \quad (45)$$

where the form factors $F_2^{\mu e}$ and $F_3^{\mu e}$ arise from the chargino, neutralino and vector bosons contributions as follows

$$F_2^{\mu e}(0) = F_{2\chi^+}^{\mu e} + F_{2\chi^0}^{\mu e} + F_{2W}^{\mu e} + F_{2Z}^{\mu e}, \quad (46)$$

$$F_3^{\mu e}(0) = F_{3\chi^+}^{\mu e} + F_{3\chi^0}^{\mu e} + F_{3W}^{\mu e} + F_{3Z}^{\mu e}. \quad (47)$$

It is also useful to define \mathcal{B}_m and \mathcal{B}_e as follows

$$\mathcal{B}_m(\mu \rightarrow e + \gamma) = \frac{24\pi^2}{G_F^2 m_\mu^2 (m_\mu + m_e)^2} |F_2^{\mu e}(0)|^2, \quad (48)$$

$$\mathcal{B}_e(\mu \rightarrow e + \gamma) = \frac{24\pi^2}{G_F^2 m_\mu^2 (m_\mu + m_e)^2} |F_3^{\mu e}(0)|^2, \quad (49)$$

where \mathcal{B}_m is the branching ratio from the magnetic dipole operator and \mathcal{B}_e is the branching ratio from the electric dipole operator. We discuss now the individual contributions to $F_2^{\mu e}$ $F_3^{\mu e}$ supersymmetric and non-supersymmetric loops.

The chargino contribution $F_{2\chi^+}^{\mu e}$ is given by

$$F_{2\chi^+}^{\mu e} = \sum_{i=1}^2 \sum_{j=1}^8 \left[\frac{m_\mu (m_\mu + m_e)}{64\pi^2 m_{\tilde{\chi}_i^+}^2} \{C_{4ij}^L C_{3ij}^{L*} + C_{4ij}^R C_{3ij}^{R*}\} F_1 \left(\frac{M_{\tilde{\nu}_j}^2}{m_{\tilde{\chi}_i^+}^2} \right) + \frac{(m_\mu + m_e)}{64\pi^2 m_{\tilde{\chi}_i^+}} \{C_{4ij}^L C_{3ij}^{R*} + C_{4ij}^R C_{3ij}^{L*}\} F_2 \left(\frac{M_{\tilde{\nu}_j}^2}{m_{\tilde{\chi}_i^+}^2} \right) \right], \quad (50)$$

where

$$F_1(x) = \frac{1}{3(x-1)^4} \{-2x^3 - 3x^2 + 6x - 1 + 6x^2 \ln x\} \quad (51)$$

and

$$F_2(x) = \frac{1}{(x-1)^3} \{3x^2 - 4x + 1 - 2x^2 \ln x\}. \quad (52)$$

The neutralino contribution $F_{2\chi^0}^{\mu e}$ is given by

$$F_{2\chi^0}^{\mu e} = \sum_{i=1}^4 \sum_{j=1}^8 \left[\frac{-m_\mu (m_\mu + m_e)}{192\pi^2 m_{\tilde{\chi}_i^0}^2} \{C_{4ij}^L C_{3ij}^{L*} + C_{4ij}^R C_{3ij}^{R*}\} F_3 \left(\frac{M_{\tilde{\tau}_j}^2}{m_{\tilde{\chi}_i^0}^2} \right) - \frac{(m_\mu + m_e)}{64\pi^2 m_{\tilde{\chi}_i^0}} \{C_{4ij}^L C_{3ij}^{R*} + C_{4ij}^R C_{3ij}^{L*}\} F_4 \left(\frac{M_{\tilde{\tau}_j}^2}{m_{\tilde{\chi}_i^0}^2} \right) \right], \quad (53)$$

where

$$F_3(x) = \frac{1}{(x-1)^4} \{-x^3 + 6x^2 - 3x - 2 - 6x \ln x\} \quad (54)$$

and

$$F_4(x) = \frac{1}{(x-1)^3} \{-x^2 + 1 + 2x \ln x\}. \quad (55)$$

The contributions from the W exchange $F_{2W}^{\mu e}$ is given by

$$F_{2W}^{\mu e} = \sum_{i=1}^4 \frac{m_\mu (m_\mu + m_e)}{32\pi^2 m_W^2} [C_{Li4}^W C_{Li3}^{W*} + C_{Ri4}^W C_{Ri3}^{W*}] F_W \left(\frac{m_{\psi_i}^2}{m_W^2} \right) + \frac{m_{\psi_i} (m_\mu + m_e)}{32\pi^2 m_W^2} [C_{Li4}^W C_{Ri3}^{W*} + C_{Ri4}^W C_{Li3}^{W*}] G_W \left(\frac{m_{\psi_i}^2}{m_W^2} \right), \quad (56)$$

where the form factors are given by

$$F_W(x) = \frac{1}{6(x-1)^4} [4x^4 - 49x^3 + 18x^3 \ln x + 78x^2 - 43x + 10] \quad (57)$$

and

$$G_W(x) = \frac{1}{(x-1)^3} [4 - 15x + 12x^2 - x^3 - 6x^2 \ln x] . \quad (58)$$

The contribution $F_{2Z}^{\mu e}$ from the Z exchange is given by

$$\begin{aligned} F_{2Z}^{\mu e} = & \sum_{\beta=1}^4 \frac{m_\mu(m_\mu + m_e)}{64\pi^2 m_Z^2} [C_{L\beta 4}^Z C_{L\beta 3}^{Z*} + C_{R\beta 4}^Z C_{R\beta 3}^{Z*}] F_Z \left(\frac{m_{\tau_\beta}^2}{m_Z^2} \right) \\ & + \frac{m_{\tau_\beta}(m_\mu + m_e)}{64\pi^2 m_Z^2} [C_{L\beta 4}^Z C_{R\beta 3}^{Z*} + C_{R\beta 4}^Z C_{L\beta 3}^{Z*}] G_Z \left(\frac{m_{\tau_\beta}^2}{m_Z^2} \right), \end{aligned} \quad (59)$$

where

$$F_Z(x) = \frac{1}{3(x-1)^4} [-5x^4 + 14x^3 - 39x^2 + 18x^2 \ln x + 38x - 8] \quad (60)$$

and

$$G_Z(x) = \frac{2}{(x-1)^3} [x^3 + 3x - 6x \ln x - 4] . \quad (61)$$

The chargino contribution $F_{3\chi^+}^{\mu e}$ is given by

$$F_{3\chi^+}^{\mu e} = \sum_{i=1}^2 \sum_{j=1}^8 \frac{(m_\mu + m_e)m_{\tilde{\chi}_i^+}}{32\pi^2 M_{\tilde{\nu}_j}^2} \{C_{4ij}^L C_{3ij}^{R*} - C_{4ij}^R C_{3ij}^{L*}\} F_5 \left(\frac{m_{\tilde{\chi}_i^+}^2}{M_{\tilde{\nu}_j}^2} \right), \quad (62)$$

where

$$F_5(x) = \frac{1}{2(x-1)^2} \left\{ -x + 3 + \frac{2 \ln x}{1-x} \right\}. \quad (63)$$

The neutralino contribution $F_{3\chi^0}^{\mu e}$ is given by

$$F_{3\chi^0}^{\mu e} = \sum_{i=1}^4 \sum_{j=1}^8 \frac{(m_\mu + m_e)m_{\tilde{\chi}_i^0}}{32\pi^2 M_{\tilde{\tau}_j}^2} \{C_{4ij}^L C_{3ij}^{R*} - C_{4ij}^R C_{3ij}^{L*}\} F_6 \left(\frac{m_{\tilde{\chi}_i^0}^2}{M_{\tilde{\tau}_j}^2} \right), \quad (64)$$

where

$$F_6(x) = \frac{1}{2(x-1)^2} \left\{ x + 1 + \frac{2x \ln x}{1-x} \right\}. \quad (65)$$

The W boson contribution $F_{3W}^{\mu e}$ is given by

$$F_{3W}^{\mu e} = - \sum_{i=1}^4 \frac{m_{\psi_i}(m_\mu + m_e)}{32\pi^2 m_W^2} [C_{Li4}^W C_{Ri3}^{W*} - C_{Ri4}^W C_{Li3}^{W*}] I_1 \left(\frac{m_{\psi_i}^2}{m_W^2} \right), \quad (66)$$

where the functions C_L^W and C_R^W are given in section 4 and the form factor I_1 is given by

$$I_1(x) = \frac{2}{(1-x)^2} \left[1 - \frac{11}{4}x + \frac{1}{4}x^2 - \frac{3x^2 \ln x}{2(1-x)} \right]. \quad (67)$$

And finally, the Z exchange diagram contribution $F_{3Z}^{\mu e}$ is given by

$$F_{3Z}^{\mu e} = \sum_{\beta=1}^4 \frac{(m_\mu + m_e) m_{\tau\beta}}{32\pi^2 m_Z^2} [C_{L4\beta}^Z C_{R3\beta}^{Z*} - C_{R4\beta}^Z C_{L3\beta}^{Z*}] I_2 \left(\frac{m_{\tau\beta}^2}{m_Z^2} \right), \quad (68)$$

where the form factor I_2 is given by

$$I_2(x) = \frac{2}{(1-x)^2} \left[1 + \frac{1}{4}x + \frac{1}{4}x^2 + \frac{3x \ln x}{2(1-x)} \right]. \quad (69)$$

6 Estimate of size of $\mathcal{B}(\mu \rightarrow e\gamma)$

In this section we give a numerical analysis for the branching ratio $\mathcal{B}(\mu \rightarrow e\gamma)$. The analysis is done in an MSSM extension with soft breaking parameters taken at the electroweak scale. Thus no renormalization group running of GUT scale parameters is needed. The parameters entering the analysis are summarized in the appendix. The scalar mass and trilinear coupling parameters are m_0 and A_0 in the slepton mass squared matrix. The corresponding ones in the sneutrino mass squared matrix are $m_0^{\tilde{\nu}}$ and $A_0^{\tilde{\nu}}$ where

$$\begin{aligned} m_0^2 &= \tilde{M}_{\tau L}^2 = \tilde{M}_E^2 = \tilde{M}_\tau^2 = \tilde{M}_\chi^2 = \tilde{M}_{\mu L}^2 = \tilde{M}_\mu^2 = \tilde{M}_{eL}^2 = \tilde{M}_e^2 \\ m_0^{\tilde{\nu}} &= \tilde{M}_N^2 = \tilde{M}_{\nu_\tau}^2 = \tilde{M}_{\nu_\mu}^2 = \tilde{M}_{\nu_e}^2 \\ A_0 &= A_\tau = A_\mu = A_e = A_E \\ A_0^{\tilde{\nu}} &= A_{\nu_\tau} = A_{\nu_\mu} = A_{\nu_e} = A_N \end{aligned} \quad (70)$$

The branching ratio $\mathcal{B}(\mu \rightarrow e\gamma)$ arises as a consequence of mixing induced by the parameters f_3, f_3', f_3'' and f_4, f_4', f_4'' where f 's are complex parameters and their arguments are the CP violating phases. The branching ratio $\mathcal{B}(\mu \rightarrow e\gamma)$ is a sensitive function of both the magnitudes as well as the phases of the mixing parameters f . We discuss the dependence of $\mathcal{B}(\mu \rightarrow e\gamma)$ on these below.

Fig. 2 exhibits the variation of $\mathcal{B}(\mu \rightarrow e\gamma)$ as a function of the CP violating phases χ_3' (left panel) and χ_3'' (right panel). As the two panels of Fig.2 show $\mathcal{B}(\mu \rightarrow e\gamma)$ is a sensitive function of these phases and can vary by an order of magnitude or more as the phases vary. The solid horizontal line gives the current experimental upper limit on $\mathcal{B}(\mu \rightarrow e\gamma)$ from the MEG experiment [1]. A very similar analysis holds when we vary the CP phases χ_4 and χ_4' as exhibited in Fig.3. Figure 4 gives the relative strength of the magnetic

and the electric dipole transition operators to $\mathcal{B}(\mu \rightarrow e\gamma)$. Thus the left panel of Fig.4 exhibits the relative strength of the contributions from the magnetic dipole operator and the electric dipole moment operator as a function of the CP phase χ_4'' . The right panel of Fig.4 exhibits the dependence of the electron EDM d_e as a function of χ_4'' where the solid horizontal line gives the current upper limit on d_e from the ACME Collaboration [25]. Thus the right panel delineates the allowed regions of the parameter space, i.e., regions consistent with the experimental upper limit constraint on d_e . The left panel of Fig.5 exhibits the variation of $\mathcal{B}(\mu \rightarrow e\gamma)$ as a function of χ_3'' for different values of the mixing parameter $|f_3''|$ while the right panel of Fig.5 gives the electric dipole moment of the electron with the horizontal solid line giving the experimental upper limit on it. A comparison of the left and the right panels show the regions of χ_3'' consistent with the current experimental upper limits on $\mathcal{B}(\mu \rightarrow e\gamma)$ and on d_e and accessible with reasonable improvement in the sensitivity of experiment in the future.

In table1 we illustrate numerically the relative strengths of the magnetic and the electric dipole transition operators to $\mathcal{B}(\mu \rightarrow e\gamma)$. Here we also show that the analysis is consistent with the current upper limits on the $\mathcal{B}(\tau \rightarrow \mu\gamma)$, on d_e and the data on the neutrino masses. Thus the current experimental limit on $\mathcal{B}(\tau \rightarrow \mu\gamma)$ is $\mathcal{B}(\tau \rightarrow \mu\gamma) < 4.4 \times 10^{-8}$ (BaBar) [26] and $\mathcal{B}(\tau \rightarrow \mu\gamma) < 4.5 \times 10^{-8}$ (Belle) [27]. Since the theoretical prediction of $\mathcal{B}(\tau \rightarrow \mu\gamma)$ in this case is smaller by several orders of magnitude than the current experimental limit this decay mode is not of imminent interest in this case. In table 2 we give a numerical analysis of the form factors F_2 and F_3 and their sub pieces arising from the supersymmetric and the non-supersymmetric loops. Also listed are \mathcal{B}_m and \mathcal{B}_e as well as d_e and the neutrino masses. One finds that typically the magnetic dipole contributions dominate the electric dipole contributions. The neutrino mass results of table 1 and table 2 are consistent with the constraint on the sum of the neutrino masses from cosmology, i.e., $\sum_i m_{\nu_i} < 0.44\text{eV}$ (95% CL) [28] and with the data on neutrino oscillations which give the neutrino mass squared differences so that [29]

$$\Delta m_{31}^2 \equiv m_3^2 - m_1^2 = 2.4_{-0.11}^{+0.12} \times 10^{-3} \text{ eV}^2 , \quad (71)$$

$$\Delta m_{21}^2 \equiv m_2^2 - m_1^2 = 7.65_{-0.20}^{+0.23} \times 10^{-5} \text{ eV}^2. \quad (72)$$

Fig. (6) exhibits a variation of $\mathcal{B}(\mu \rightarrow e\gamma)$ as a function of the mirror masses m_E and m_N . All points of the four curves of Fig. (6) are consistent with the constraints set on the neutrino masses by eq. (71) and (72). We note that in the analysis of Fig. (2)- Fig.(4) the mass parameters are typically low. For instance in the analysis of Fig.4 we have used $|\mu| = 310 \text{ GeV}$, $M_1 = 180 \text{ GeV}$ and $M_2 = 140 \text{ GeV}$ and our vectorlike masses are chosen so that $m_E = m_N = 150, 200, 250, 300$. Such a choice may be close to the LHC exclusion plots based on LHC RUN I data and could be close to being probed with more data. We should note that the LHC particle searches are very model dependent as can be seen from the analyses of [31, 32]. For instance in the

ATLAS analysis of [32] the lightest chargino mass is excluded up to 700 GeV, 380 GeV, 345 GeV or 148 GeV for a massless neutralino depending on the allowed decay channels. These results would be even more model dependent if the neutralino is assumed massive with a varying mass. Thus while the current limits from LHC do not directly apply to our analysis, the choice of low mass parameters point to the possibility that they could be probed in RUN II of the LHC. It would thus be very interesting to carryout a signal analysis of this model specifically, for instance, for multilepton searches. Such an analysis, however, is beyond the scope of this paper.

7 Conclusion

In this work we have given an analysis of $\mu \rightarrow e\gamma$ decay with inclusion of a vectorlike leptonic generation where mixings appear between leptons and mirror leptons as well as between sleptons and mirror sleptons. The decay $\mu \rightarrow e\gamma$ arises from diagrams with charginos and sneutrinos and mirror sneutrinos, and neutralinos, sleptons and mirror sleptons in the loops. Additionally electroweak loops are included where W, Z and leptons and mirror leptons and neutrinos are exchanged. An analytic analysis of these contributions is given in section 5 while a detailed numerical analysis is given in section 6. Here it is shown that the current experimental limits from the MEG experiment put constraints on the parameter space of models. Further, the size of the new contributions are such that improvement in experiment will either reveal new physics or the improved experimental results will be able to probe large parts of the parameter space of the extended MSSM model. Thus the MEG experiment is continuing to collect data and is expected to explore the $\mu \rightarrow e + \gamma$ decay down to a branching ratio sensitivity of a few times 10^{-13} in the next few years. This will allow a further probe of this new class of MSSM extensions.

Acknowledgments: PN's research is supported in part by the NSF grant PHY-1314774.

8 Appendix: The scalar mass squared matrices

For convenience we collect here all the contributions to the scalar mass squared matrices arising from the F terms. They are given by

$$\mathcal{L}_F^{\text{mass}} = \mathcal{L}_C^{\text{mass}} + \mathcal{L}_N^{\text{mass}}, \quad (73)$$

where $\mathcal{L}_C^{\text{mass}}$ gives the mass terms for the charged sleptons while $\mathcal{L}_N^{\text{mass}}$ gives the mass terms for the sneutrinos.

For $\mathcal{L}_C^{\text{mass}}$ we have

$$\begin{aligned}
-\mathcal{L}_C^{\text{mass}} = & \left(\frac{v_2^2 |f_2'|^2}{2} + |f_3|^2 + |f_3'|^2 + |f_3''|^2 \right) \tilde{E}_R \tilde{E}_R^* + \left(\frac{v_2^2 |f_2'|^2}{2} + |f_4|^2 + |f_4'|^2 + |f_4''|^2 \right) \tilde{E}_L \tilde{E}_L^* \\
& + \left(\frac{v_1^2 |f_1|^2}{2} + |f_4|^2 \right) \tilde{\tau}_R \tilde{\tau}_R^* + \left(\frac{v_1^2 |f_1|^2}{2} + |f_3|^2 \right) \tilde{\tau}_L \tilde{\tau}_L^* + \left(\frac{v_1^2 |h_1|^2}{2} + |f_4|^2 \right) \tilde{\mu}_R \tilde{\mu}_R^* \\
& + \left(\frac{v_1^2 |h_1|^2}{2} + |f_3|^2 \right) \tilde{\mu}_L \tilde{\mu}_L^* + \left(\frac{v_1^2 |h_2|^2}{2} + |f_4''|^2 \right) \tilde{e}_R \tilde{e}_R^* + \left(\frac{v_1^2 |h_2|^2}{2} + |f_3''|^2 \right) \tilde{e}_L \tilde{e}_L^* \\
& + \left\{ -\frac{f_1 \mu^* v_2}{\sqrt{2}} \tilde{\tau}_L \tilde{\tau}_R^* - \frac{h_1 \mu^* v_2}{\sqrt{2}} \tilde{\mu}_L \tilde{\mu}_R^* - \frac{f_2' \mu^* v_1}{\sqrt{2}} \tilde{E}_L \tilde{E}_R^* + \left(\frac{f_2' v_2 f_3^*}{\sqrt{2}} + \frac{f_4 v_1 f_1^*}{\sqrt{2}} \right) \tilde{E}_L \tilde{\tau}_L^* \right. \\
& + \left(\frac{f_4 v_2 f_2'^*}{\sqrt{2}} + \frac{f_1 v_1 f_3^*}{\sqrt{2}} \right) \tilde{E}_R \tilde{\tau}_R^* + \left(\frac{f_3' v_2 f_2'^*}{\sqrt{2}} + \frac{h_1 v_1 f_4^*}{\sqrt{2}} \right) \tilde{E}_L \tilde{\mu}_L^* + \left(\frac{f_2' v_2 f_4^*}{\sqrt{2}} + \frac{f_3' v_1 h_1^*}{\sqrt{2}} \right) \tilde{E}_R \tilde{\mu}_R^* \\
& + \left(\frac{f_3'' v_2 f_2'}{\sqrt{2}} + \frac{f_4'' v_1 h_2^*}{\sqrt{2}} \right) \tilde{E}_L \tilde{e}_L^* + \left(\frac{f_4'' v_2 f_2'}{\sqrt{2}} + \frac{f_3'' v_1 h_2^*}{\sqrt{2}} \right) \tilde{E}_R \tilde{e}_R^* + f_3' f_3^* \tilde{\mu}_L \tilde{\tau}_L^* + f_4 f_4^* \tilde{\mu}_R \tilde{\tau}_R^* \\
& \left. + f_4 f_4^* \tilde{e}_R \tilde{\tau}_R^* + f_3'' f_3^* \tilde{e}_L \tilde{\tau}_L^* + f_3'' f_3^* \tilde{e}_L \tilde{\mu}_L^* + f_4' f_4'' \tilde{e}_R \tilde{\mu}_R^* - \frac{h_2 \mu^* v_2}{\sqrt{2}} \tilde{e}_L \tilde{e}_R^* + H.c. \right\}. \tag{74}
\end{aligned}$$

We define the scalar mass squared matrix M_τ^2 in the basis $(\tilde{\tau}_L, \tilde{E}_L, \tilde{\tau}_R, \tilde{E}_R, \tilde{\mu}_L, \tilde{\mu}_R, \tilde{e}_L, \tilde{e}_R)$. We label the matrix elements of these as $(M_\tau^2)_{ij} = M_{ij}^2$ where the elements of the matrix are given by

$$\begin{aligned}
M_{11}^2 &= \tilde{M}_{\tau_L}^2 + \frac{v_1^2 |f_1|^2}{2} + |f_3|^2 - m_Z^2 \cos 2\beta \left(\frac{1}{2} - \sin^2 \theta_W \right), \\
M_{22}^2 &= \tilde{M}_E^2 + \frac{v_2^2 |f_2'|^2}{2} + |f_4|^2 + |f_4'|^2 + |f_4''|^2 + m_Z^2 \cos 2\beta \sin^2 \theta_W, \\
M_{33}^2 &= \tilde{M}_\tau^2 + \frac{v_1^2 |f_1|^2}{2} + |f_4|^2 - m_Z^2 \cos 2\beta \sin^2 \theta_W, \\
M_{44}^2 &= \tilde{M}_\chi^2 + \frac{v_2^2 |f_2'|^2}{2} + |f_3|^2 + |f_3'|^2 + |f_3''|^2 + m_Z^2 \cos 2\beta \left(\frac{1}{2} - \sin^2 \theta_W \right), \\
M_{55}^2 &= \tilde{M}_{\mu_L}^2 + \frac{v_1^2 |h_1|^2}{2} + |f_3|^2 - m_Z^2 \cos 2\beta \left(\frac{1}{2} - \sin^2 \theta_W \right), \\
M_{66}^2 &= \tilde{M}_\mu^2 + \frac{v_1^2 |h_1|^2}{2} + |f_4|^2 - m_Z^2 \cos 2\beta \sin^2 \theta_W, \\
M_{77}^2 &= \tilde{M}_{e_L}^2 + \frac{v_1^2 |h_2|^2}{2} + |f_3''|^2 - m_Z^2 \cos 2\beta \left(\frac{1}{2} - \sin^2 \theta_W \right), \\
M_{88}^2 &= \tilde{M}_e^2 + \frac{v_1^2 |h_2|^2}{2} + |f_4''|^2 - m_Z^2 \cos 2\beta \sin^2 \theta_W.
\end{aligned}$$

$$\begin{aligned}
M_{12}^2 &= M_{21}^{2*} = \frac{v_2 f_2' f_3^*}{\sqrt{2}} + \frac{v_1 f_4 f_1^*}{\sqrt{2}}, M_{13}^2 = M_{31}^{2*} = \frac{f_1^*}{\sqrt{2}}(v_1 A_\tau^* - \mu v_2), M_{14}^2 = M_{41}^{2*} = 0, \\
M_{15}^2 &= M_{51}^{2*} = f_3' f_3^*, M_{16}^2 = M_{61}^{2*} = 0, M_{17}^2 = M_{71}^{2*} = f_3'' f_3^*, M_{18}^2 = M_{81}^{2*} = 0, \\
M_{23}^2 &= M_{32}^{2*} = 0, M_{24}^2 = M_{42}^{2*} = \frac{f_2^*}{\sqrt{2}}(v_2 A_E^* - \mu v_1), M_{25}^2 = M_{52}^{2*} = \frac{v_2 f_3' f_2^*}{\sqrt{2}} + \frac{v_1 h_1 f_4^*}{\sqrt{2}}, \\
M_{26}^2 &= M_{62}^{2*} = 0, M_{27}^2 = M_{72}^{2*} = \frac{v_2 f_3'' f_2^*}{\sqrt{2}} + \frac{v_1 h_2 f_4^*}{\sqrt{2}}, M_{28}^2 = M_{82}^{2*} = 0, \\
M_{34}^2 &= M_{43}^{2*} = \frac{v_2 f_4 f_2^*}{\sqrt{2}} + \frac{v_1 f_1 f_3^*}{\sqrt{2}}, M_{35}^2 = M_{53}^{2*} = 0, M_{36}^2 = M_{63}^{2*} = f_4 f_4^*, \\
M_{37}^2 &= M_{73}^{2*} = 0, M_{38}^2 = M_{83}^{2*} = f_4 f_4^*, \\
M_{45}^2 &= M_{54}^{2*} = 0, M_{46}^2 = M_{64}^{2*} = \frac{v_2 f_2' f_4^*}{\sqrt{2}} + \frac{v_1 f_3' h_1^*}{\sqrt{2}}, \\
M_{47}^2 &= M_{74}^{2*} = 0, M_{48}^2 = M_{84}^{2*} = \frac{v_2 f_2' f_4^*}{\sqrt{2}} + \frac{v_1 f_3'' h_2^*}{\sqrt{2}}, \\
M_{56}^2 &= M_{65}^{2*} = \frac{h_1^*}{\sqrt{2}}(v_1 A_\mu^* - \mu v_2), M_{57}^2 = M_{75}^{2*} = f_3'' f_3^*, \\
M_{58}^2 &= M_{85}^{2*} = 0, M_{67}^2 = M_{76}^{2*} = 0, \\
M_{68}^2 &= M_{86}^{2*} = f_4' f_4^*, M_{78}^2 = M_{87}^{2*} = \frac{h_2^*}{\sqrt{2}}(v_1 A_e^* - \mu v_2).
\end{aligned}$$

We can diagonalize this hermitian mass squared matrix by the unitary transformation

$$\tilde{D}^{\tau\dagger} M_{\tilde{\tau}}^2 \tilde{D}^\tau = \text{diag}(M_{\tilde{\tau}_1}^2, M_{\tilde{\tau}_2}^2, M_{\tilde{\tau}_3}^2, M_{\tilde{\tau}_4}^2, M_{\tilde{\tau}_5}^2, M_{\tilde{\tau}_6}^2, M_{\tilde{\tau}_7}^2, M_{\tilde{\tau}_8}^2). \quad (75)$$

For $\mathcal{L}_N^{\text{mass}}$ we have

$$\begin{aligned}
-\mathcal{L}_N^{\text{mass}} = & \left(\frac{v_1^2 |f_2|^2}{2} + |f_3|^2 + |f_3'|^2 + |f_3''|^2 \right) \tilde{N}_R \tilde{N}_R^* \\
& + \left(\frac{v_1^2 |f_2|^2}{2} + |f_5|^2 + |f_5'|^2 + |f_5''|^2 \right) \tilde{N}_L \tilde{N}_L^* + \left(\frac{v_2^2 |f_1'|^2}{2} + |f_5|^2 \right) \tilde{\nu}_{\tau R} \tilde{\nu}_{\tau R}^* \\
& + \left(\frac{v_2^2 |f_1|^2}{2} + |f_3|^2 \right) \tilde{\nu}_{\tau L} \tilde{\nu}_{\tau L}^* + \left(\frac{v_2^2 |h_1'|^2}{2} + |f_3'|^2 \right) \tilde{\nu}_{\mu L} \tilde{\nu}_{\mu L}^* + \left(\frac{v_2^2 |h_1|^2}{2} + |f_5|^2 \right) \tilde{\nu}_{\mu R} \tilde{\nu}_{\mu R}^* \\
& + \left(\frac{v_2^2 |h_2|^2}{2} + |f_3''|^2 \right) \tilde{\nu}_{eL} \tilde{\nu}_{eL}^* + \left(\frac{v_2^2 |h_2'|^2}{2} + |f_5''|^2 \right) \tilde{\nu}_{eR} \tilde{\nu}_{eR}^* \\
& + \left\{ -\frac{f_2 \mu^* v_2}{\sqrt{2}} \tilde{N}_L \tilde{N}_R^* - \frac{f_1' \mu^* v_1}{\sqrt{2}} \tilde{\nu}_{\tau L} \tilde{\nu}_{\tau R}^* - \frac{h_1' \mu^* v_1}{\sqrt{2}} \tilde{\nu}_{\mu L} \tilde{\nu}_{\mu R}^* + \left(\frac{f_5 v_2 f_1^*}{\sqrt{2}} - \frac{f_2 v_1 f_3^*}{\sqrt{2}} \right) \tilde{N}_L \tilde{\nu}_{\tau L}^* \right. \\
& + \left(\frac{f_5 v_1 f_2^*}{\sqrt{2}} - \frac{f_1' v_2 f_3^*}{\sqrt{2}} \right) \tilde{N}_R \tilde{\nu}_{\tau R}^* + \left(\frac{h_1' v_2 f_5^*}{\sqrt{2}} - \frac{f_3' v_1 f_2^*}{\sqrt{2}} \right) \tilde{N}_L \tilde{\nu}_{\mu L}^* + \left(\frac{f_5'' v_1 f_2^*}{\sqrt{2}} - \frac{f_3'' v_2 h_2^*}{\sqrt{2}} \right) \tilde{N}_R \tilde{\nu}_{eR}^* \\
& + \left(\frac{h_2^* v_2 f_5''}{\sqrt{2}} - \frac{f_3'' v_1 f_2}{\sqrt{2}} \right) \tilde{N}_L \tilde{\nu}_{eL}^* + \left(\frac{f_5' v_1 f_2^*}{\sqrt{2}} - \frac{h_1' v_2 f_3^*}{\sqrt{2}} \right) \tilde{N}_R \tilde{\nu}_{\mu R}^* \\
& \left. + f_3' f_3^* \tilde{\nu}_{\mu L} \tilde{\nu}_{\tau L}^* + f_5 f_5^* \tilde{\nu}_{\mu R} \tilde{\nu}_{\tau R}^* - \frac{h_2' \mu^* v_1}{\sqrt{2}} \tilde{\nu}_{eL} \tilde{\nu}_{eR}^* \right. \\
& \left. + f_3'' f_3^* \tilde{\nu}_{eL} \tilde{\nu}_{\tau L}^* + f_5 f_5^* \tilde{\nu}_{eR} \tilde{\nu}_{\tau R}^* + f_3'' f_3^* \tilde{\nu}_{eL} \tilde{\nu}_{\mu L}^* + f_5' f_5^* \tilde{\nu}_{eR} \tilde{\nu}_{\mu R}^* + H.c. \right\}.
\end{aligned}$$

Next we write the mass squared matrix in the sneutrino sector the basis $(\tilde{\nu}_{\tau L}, \tilde{N}_L, \tilde{\nu}_{\tau R}, \tilde{N}_R, \tilde{\nu}_{\mu L}, \tilde{\nu}_{\mu R}, \tilde{\nu}_{eL}, \tilde{\nu}_{eR})$.

Thus here we denote the sneutrino mass squared matrix in the form $(M_{\tilde{\nu}}^2)_{ij} = m_{ij}^2$ where

$$\begin{aligned}
m_{11}^2 &= \tilde{M}_{\tau L}^2 + \frac{v_2^2 |f_1'|^2}{2} + |f_3|^2 + \frac{1}{2} m_Z^2 \cos 2\beta, \\
m_{22}^2 &= \tilde{M}_N^2 + \frac{v_1^2 |f_2|^2}{2} + |f_5|^2 + |f_5'|^2 + |f_5''|^2, \\
m_{33}^2 &= \tilde{M}_{\nu_\tau}^2 + \frac{v_2^2 |h_1'|^2}{2} + |f_5|^2, \\
m_{44}^2 &= \tilde{M}_\chi^2 + \frac{v_2^2 |f_2|^2}{2} + |f_3|^2 + |f_3'|^2 + |f_3''|^2 - \frac{1}{2} m_Z^2 \cos 2\beta, \\
m_{55}^2 &= \tilde{M}_{\mu L}^2 + \frac{v_2^2 |f_1'|^2}{2} + |f_3|^2 + \frac{1}{2} m_Z^2 \cos 2\beta, \\
m_{66}^2 &= \tilde{M}_{\nu_\mu}^2 + \frac{v_2^2 |h_1|^2}{2} + |f_5|^2, \\
m_{77}^2 &= \tilde{M}_{eL}^2 + \frac{v_2^2 |h_2|^2}{2} + |f_3''|^2 + \frac{1}{2} m_Z^2 \cos 2\beta, \\
m_{88}^2 &= \tilde{M}_{\nu_e}^2 + \frac{v_2^2 |h_2'|^2}{2} + |f_5''|^2,
\end{aligned}$$

$$\begin{aligned}
m_{12}^2 &= m_{21}^{2*} = \frac{v_2 f_5 f_1'^*}{\sqrt{2}} - \frac{v_1 f_2 f_3^*}{\sqrt{2}}, \quad m_{13}^2 = m_{31}^{2*} = \frac{f_1'^*}{\sqrt{2}}(v_2 A_{\nu\tau}^* - \mu v_1), \\
m_{14}^2 &= m_{41}^{2*} = 0, \quad m_{15}^2 = m_{51}^{2*} = f_3' f_3^*, \quad m_{16}^2 = m_{61}^{2*} = 0, \\
m_{17}^2 &= m_{71}^{2*} = f_3'' f_3^*, \quad m_{18}^2 = m_{81}^{2*} = 0, \\
m_{23}^2 &= m_{32}^{2*} = 0, \quad m_{24}^2 = m_{42}^{2*} = \frac{f_2^*}{\sqrt{2}}(v_1 A_N^* - \mu v_2), \\
m_{25}^2 &= m_{52}^{2*} = -\frac{v_1 f_2^* f_3'}{\sqrt{2}} + \frac{h_1' v_2 f_5'^*}{\sqrt{2}}, \\
m_{26}^2 &= m_{62}^{2*} = 0, \quad m_{27}^2 = m_{72}^{2*} = -\frac{v_1 f_2^* f_3''}{\sqrt{2}} + \frac{h_2' v_2 f_5''^*}{\sqrt{2}}, \\
m_{28}^2 &= m_{82}^{2*} = 0, \quad m_{34}^2 = m_{43}^{2*} = \frac{v_1 f_2^* f_5}{\sqrt{2}} - \frac{v_2 f_1' f_3^*}{\sqrt{2}}, \\
m_{35}^2 &= m_{53}^{2*} = 0, \quad m_{36}^2 = m_{63}^{2*} = f_5 f_5'^*, \\
m_{37}^2 &= m_{73}^{2*} = 0, \quad m_{38}^2 = m_{83}^{2*} = f_5 f_5''^*, \\
m_{45}^2 &= m_{54}^{2*} = 0, \quad m_{46}^2 = m_{64}^{2*} = -\frac{h_1'^* v_2 f_3'}{\sqrt{2}} + \frac{v_1 f_2 f_5'^*}{\sqrt{2}}, \\
m_{47}^2 &= m_{74}^{2*} = 0, \quad m_{48}^2 = m_{84}^{2*} = \frac{v_1 f_2 f_5''^*}{\sqrt{2}} - \frac{v_2 h_2'^* f_3''}{\sqrt{2}}, \\
m_{56}^2 &= m_{65}^{2*} = \frac{h_1'^*}{\sqrt{2}}(v_2 A_{\nu\mu}^* - \mu v_1), \\
m_{57}^2 &= m_{75}^{2*} = f_3'' f_3'^*, \quad m_{58}^2 = m_{85}^{2*} = 0, \\
m_{67}^2 &= m_{76}^{2*} = 0, \quad m_{68}^2 = m_{86}^{2*} = f_5' f_5''^*, \\
m_{78}^2 &= m_{87}^{2*} = \frac{h_2'^*}{\sqrt{2}}(v_2 A_{\nu e}^* - \mu v_1). \tag{76}
\end{aligned}$$

We can diagonalize the sneutrino mass square matrix by the unitary transformation

$$\tilde{D}^{\nu\dagger} M_{\tilde{\nu}}^2 \tilde{D}^{\nu} = \text{diag}(M_{\tilde{\nu}_1}^2, M_{\tilde{\nu}_2}^2, M_{\tilde{\nu}_3}^2, M_{\tilde{\nu}_4}^2, M_{\tilde{\nu}_5}^2, M_{\tilde{\nu}_6}^2, M_{\tilde{\nu}_7}^2, M_{\tilde{\nu}_8}^2). \tag{77}$$

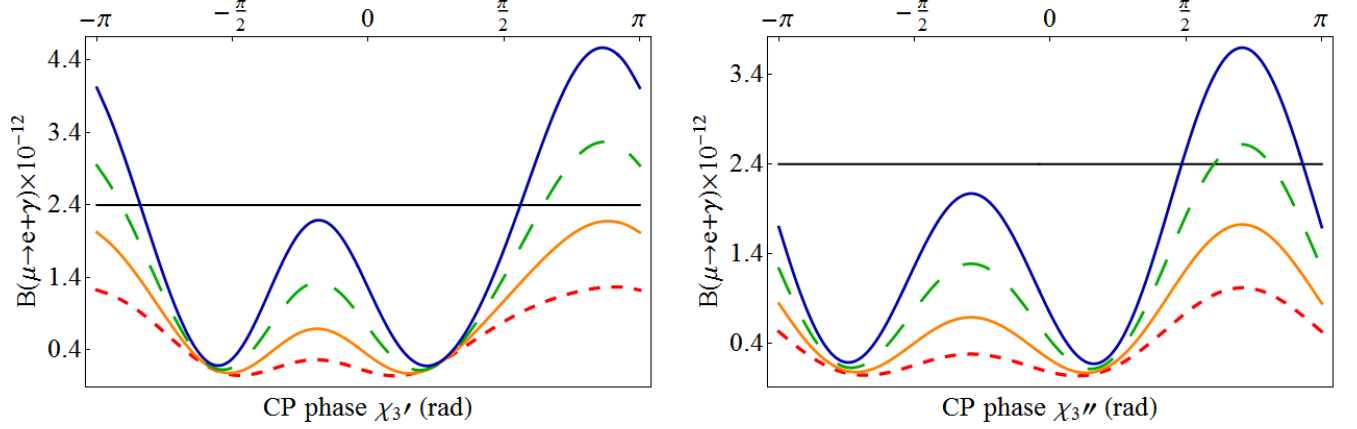


Figure 2: Left Panel: An exhibition of the dependence of $\mathcal{B}(\mu \rightarrow e\gamma)$ on χ_3' where $\chi_3 = \chi_3'' = \chi_3'$. The $\mathcal{B}(\mu \rightarrow e\gamma)$ curves (bottom to top at $\chi_3' = \pi$) are for the cases when $|f_3| = |f_3'| = |f_3''| = 5 \times 10^{-5}$, 7×10^{-5} , 9×10^{-5} , and 11×10^{-5} . Right Panel: An exhibition of $\mathcal{B}(\mu \rightarrow e\gamma)$ as a function of the χ_3'' where the curves (bottom to top at $\chi_3'' = \pi$) are for the cases $|f_3| = 5 \times 10^{-5}$, 7×10^{-5} , 9×10^{-5} , 11×10^{-5} where $|f_3| = |f_3'| = 5 \times 10^{-5}$ and $\chi_3 = \chi_3' = 0.3$. The common parameters for both panels are $\tan \beta = 5$, $|\mu| = 500$, $|M_1| = 130$, $|M_2| = 110$, $m_N = 260$, $m_E = 280$, $m_0 = 4 \times 10^5$, $m_0^{\tilde{\nu}} = 5 \times 10^5$, $|A_0| = |A_0^{\tilde{\nu}}| = 6 \times 10^5$, $\alpha_1 = 0.4$, $\alpha_2 = \alpha_\mu = 0.5$, $\alpha_{A_0} = \alpha_{A_0^{\tilde{\nu}}} = 1$, $|f_4| = |f_4'| = 1$, $|f_4''| = 0.1$, $|f_5| = 3 \times 10^{-6}$, $|f_5'| = 8 \times 10^{-7}$, $|f_5''| = 5 \times 10^{-6}$, $\chi_4 = 1$, $\chi_4' = \chi_4'' = 0.5$, $\chi_5 = \chi_5' = \chi_5'' = 1$. The solid horizontal line is the upper limit from the MEG experiment [1]. Here and in the rest of the figures and in the tables all masses are in GeV and phase angles in radian.

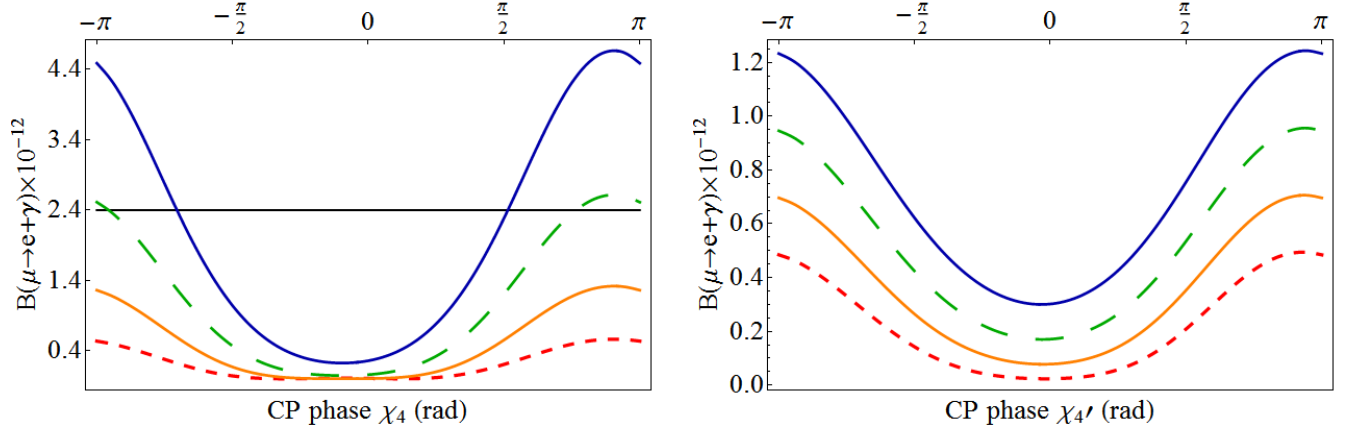


Figure 3: Left Panel: Plot of $\mathcal{B}(\mu \rightarrow e\gamma)$ as a function of χ_4 when $\chi_4' = \chi_4'' = \chi_4$. The curves from bottom to top at $\chi_4 = \pi$ are for the cases $|f_4| = |f_4'| = |f_4''| = 0.1$, 0.5 , 1 , and 1.5 and $|f_3| = |f_3'| = |f_3''| = 5 \times 10^{-5}$ and $\chi_3 = \chi_3' = \chi_3'' = 0.3$. The solid horizontal line is the upper limit from the MEG experiment [1]. Right Panel: An exhibition of the dependence of $\mathcal{B}(\mu \rightarrow e\gamma)$ on χ_4' . The curves from bottom to top at $\chi_4' = \pi$ are for the cases when $|f_4'| = 0.3$, 0.4 , 0.5 , and 0.6 and $|f_4| = |f_4''| = 0.4$, $\chi_4 = \chi_4'' = 1$. All other parameters in both panels are the same as in Fig.2.

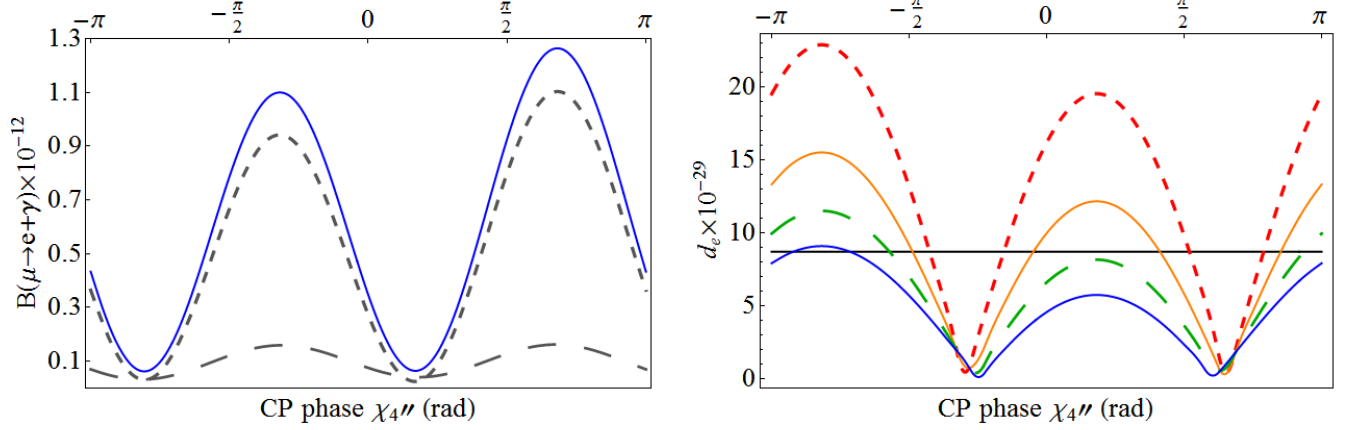


Figure 4: Left Panel: An exhibition of the magnetic contribution \mathcal{B}_m (dotted) as given by Eq. (48), the electric contribution \mathcal{B}_e (dashed) as given by Eq. (49) to $\mathcal{B}(\mu \rightarrow e\gamma)$ where the solid curve stands for their sum as a function of χ_4'' when $m_E = m_N = 300$. Right Panel: An exhibition of d_e as a function of χ_4'' . The curves from top to bottom at $\chi_4'' = \pi$ are for values of $m_E = m_N = 150, 200, 250$, and 300 . The solid horizontal line is the upper limit on d_e from the ACME Collaboration [25]. The common parameters for the two panels are $|\mu| = 310$, $|M_1| = 180$, $|M_2| = 140$, $\tan\beta = 20$, $m_0 = 4 \times 10^5$, $|A_0| = 1.5 \times 10^6$, $m_0^{\tilde{\nu}} = 4 \times 10^5$, $|A_0^{\tilde{\nu}}| = 5.1 \times 10^6$, $\alpha_1 = 0.4$, $\alpha_2 = 0.2$, $\alpha_\mu = 0.7$, $\alpha_{A_0} = \alpha_{A_0^{\tilde{\nu}}} = 1$. The mixings are $|f_3| = 7 \times 10^{-4}$, $|f_3'| = 1 \times 10^{-4}$, $|f_3''| = 2 \times 10^{-4}$, $|f_4| = 3 \times 10^{-2}$, $|f_4'| = 0.4$, $|f_4''| = 5 \times 10^{-2}$, $|f_5| = 3.8 \times 10^{-6}$, $|f_5'| = 2.2 \times 10^{-6}$, $|f_5''| = 3 \times 10^{-6}$, $\chi_3 = \chi_3' = \chi_3'' = 1$, $\chi_4 = 0.3$, $\chi_4' = 0.2$, $\chi_5 = \chi_5' = \chi_5'' = 0.5$.

	(i) $m_E = m_N = 300$	(ii) $m_E = m_N = 150$
\mathcal{B}_m	1.1×10^{-12}	8.3×10^{-12}
\mathcal{B}_e	1.6×10^{-13}	1.2×10^{-12}
$\mathcal{B}(\mu \rightarrow e\gamma)$	1.2×10^{-12}	9.4×10^{-12}
$\mathcal{B}(\tau \rightarrow \mu\gamma)$	4.8×10^{-25}	8.0×10^{-25}
d_e (ecm)	6.3×10^{-30}	1.3×10^{-29}
$m_{\nu 3}$	5.0×10^{-11}	5.5×10^{-11}
$m_{\nu 2}$	8.9×10^{-12}	9.6×10^{-12}
$m_{\nu 1}$	1.1×10^{-12}	2.5×10^{-12}

Table 1: An exhibition of the numerical values of \mathcal{B}_m , \mathcal{B}_e , $\mathcal{B}(\mu \rightarrow e\gamma)$ and $\mathcal{B}(\tau \rightarrow \mu + \gamma)$ when $\chi_4'' = 2$ for two values of $m_E = m_N$ while other parameters are the same as in Fig.4. The values of the electron EDM d_e and the neutrino masses $m_{\nu 1}, m_{\nu 2}, m_{\nu 3}$ are also exhibited.

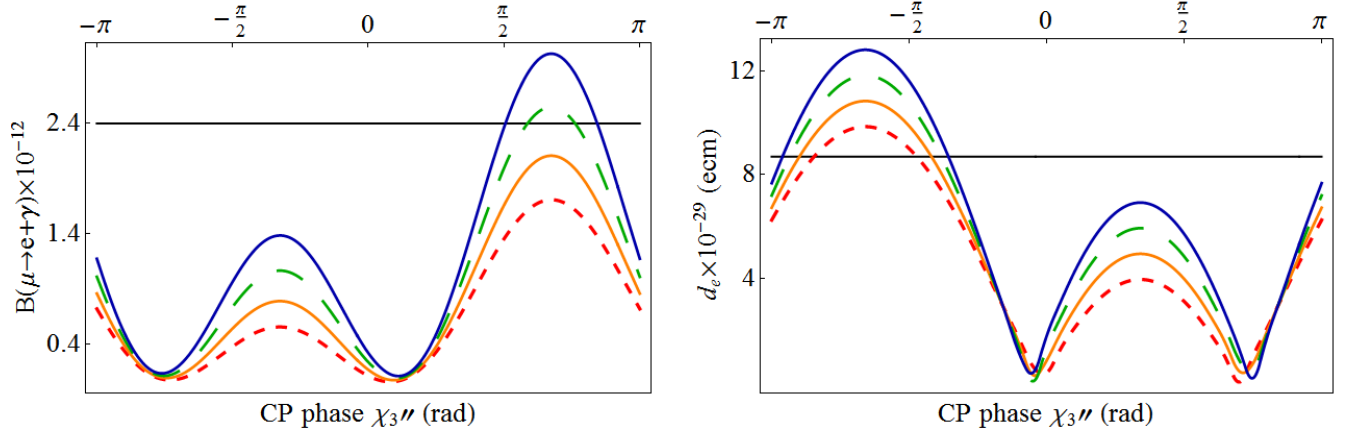


Figure 5: Left Panel: A plot of $\mathcal{B}(\mu \rightarrow e\gamma)$ as a function of χ_3'' where the curves from bottom to top at $\chi_3'' = 2$ are for values of $|f_3''| = 7 \times 10^{-5}, 8 \times 10^{-5}, 9 \times 10^{-5}, 1 \times 10^{-4}$. The solid horizontal line is the upper limit from the MEG experiment [1]. Right Panel: Plot of d_e as a function of χ_3'' for the same values of f_3'' as in the left panel. The solid horizontal line is the upper limit on d_e from the ACME Collaboration [25]. The parameters used are $\tan \beta = 5$, $|\mu| = 500$, $|M_1| = 130$, $|M_2| = 110$, $m_N = 260$, $m_E = 240$, $m_0 = 7 \times 10^4$, $m_0^{\tilde{\nu}} = 5 \times 10^4$, $|A_0| = |A_0^{\tilde{\nu}}| = 6 \times 10^5$, $\alpha_1 = 0.4$, $\alpha_2 = \alpha_\mu = 0.5$, $\alpha_{A_0} = \alpha_{A_0^{\tilde{\nu}}} = 1$. The mixings are $|f_3| = 3 \times 10^{-5}$, $|f_3'| = 4 \times 10^{-6}$, $|f_4| = |f_4'| = 0.8$, $|f_4''| = 0.1$, $|f_5| = 3 \times 10^{-6}$, $|f_5'| = 7 \times 10^{-6}$, $|f_5''| = 5 \times 10^{-6}$. Their CP phases are $\chi_3 = 0.3$, $\chi_3' = 0.4$, $\chi_4 = 1$, $\chi_4' = \chi_4'' = 0.5$, $\chi_5 = \chi_5' = \chi_5'' = 1$.

	(i) $\chi_3'' = 0.39$	(ii) $\chi_3'' = 2.1$
$F_{2\chi^+}^{\mu e}$	$2.7 \times 10^{-18} e^{-0.74i}$	$2.8 \times 10^{-18} e^{-2.1i}$
$F_{2\chi^0}^{\mu e}$	$3.4 \times 10^{-21} e^{0.56i}$	$3.5 \times 10^{-21} e^{-0.39i}$
$F_{2W}^{\mu e}$	$5.8 \times 10^{-15} e^{-1.5i}$	$6.1 \times 10^{-15} e^{0.12i}$
$F_{2Z}^{\mu e}$	$4.0 \times 10^{-15} e^{1.4i}$	$4.7 \times 10^{-15} e^{-0.15i}$
$F_2^{\mu e}(0)$	$1.9 \times 10^{-15} e^{-1.1i}$	$1.1 \times 10^{-14} e^{0.0024i}$
\mathcal{B}_m	5.3×10^{-14}	5.6×10^{-13}
$F_{3\chi^+}^{\mu e}$	$2.4 \times 10^{-18} e^{3.04i}$	$9.5 \times 10^{-19} e^{0.45i}$
$F_{3\chi^0}^{\mu e}$	$1.3 \times 10^{-20} e^{0.53i}$	$1.6 \times 10^{-21} e^{-1.1i}$
$F_{3W}^{\mu e}$	$3.3 \times 10^{-15} e^{-1.7i}$	$2.3 \times 10^{-15} e^{-0.019i}$
$F_{3Z}^{\mu e}$	$1.5 \times 10^{-15} e^{1.9i}$	$5.8 \times 10^{-16} e^{0.34i}$
$F_3^{\mu e}(0)$	$2.2 \times 10^{-15} e^{-2.1i}$	$2.9 \times 10^{-15} e^{0.051i}$
\mathcal{B}_e	6.6×10^{-14}	6.7×10^{-14}
$\mathcal{B}(\mu \rightarrow e\gamma)$	1.2×10^{-13}	1.7×10^{-12}
$\mathcal{B}(\tau \rightarrow \mu\gamma)$	2.5×10^{-19}	2.5×10^{-19}
d_e (ecm)	4.7×10^{-29}	6.1×10^{-30}
$m_{\nu 3}$	4.7×10^{-11}	4.7×10^{-11}
$m_{\nu 2}$	9.1×10^{-12}	8.8×10^{-12}
$m_{\nu 1}$	2.1×10^{-12}	4.9×10^{-13}

Table 2: An exhibition of the numerical values of the form factors $F_2^{\mu e}$ and $F_3^{\mu e}$ and their sub pieces for two cases: (i) and (ii). For case (i) $|f_3''| = 10^{-4}$ and $\chi_3'' = 0.39$ while for case (ii) $|f_3''| = 0.7 \times 10^{-4}$ and $\chi_3'' = 2.1$. All other parameters used in this table are the same as Fig.5. The magnetic and electric transition operators \mathcal{B}_m and \mathcal{B}_e are also listed as are d_e and the neutrino mass eigenstates for each case listed above.

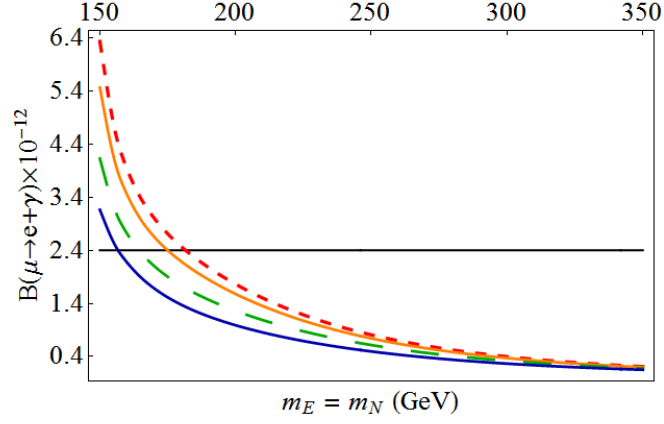


Figure 6: A plot of $\mathcal{B}(\mu \rightarrow e\gamma)$ as a function of $m_E = m_N$ where the curves from top to bottom at $m_E = m_N = 150$ are for values of $|f_4| = 0.1, 0.5, 1, 1.5$. The parameters used are $|\mu| = 500$, $|M_1| = 130$, $|M_2| = 110$, $\tan\beta = 10$, $m_0 = 4 \times 10^4$, $|A_0| = 6 \times 10^5$, $m_0^{\tilde{\nu}} = 5 \times 10^4$, $|A_0^{\tilde{\nu}}| = 6 \times 10^5$, $\alpha_1 = 0.4$, $\alpha_2 = 0.5$, $\alpha_\mu = 0.5$, $\alpha_{A_0} = \alpha_{A_0^{\tilde{\nu}}} = 0.6$. The mixings are $|f_3| = 5 \times 10^{-5}$, $|f'_3| = 5 \times 10^{-5}$, $|f''_3| = 5 \times 10^{-5}$, $|f'_4| = 0.5$, $|f''_4| = 5 \times 10^{-1}$, $|f_5| = 3 \times 10^{-6}$, $|f'_5| = 8 \times 10^{-7}$, $|f''_5| = 5 \times 10^{-6}$, $\chi_3 = \chi'_3 = \chi''_3 = 0.3$, $\chi_4 = \chi'_4 = \chi''_4 = 1$, $\chi_5 = \chi'_5 = \chi''_5 = 1$.

References

- [1] J. Adam *et al.* [MEG Collaboration], Phys. Rev. Lett. **107**, 171801 (2011) [arXiv:1107.5547 [hep-ex]].
- [2] H. Georgi, “Towards A Grand Unified Theory Of Flavor,” Nucl. Phys. B **156**, 126 (1979); F. Wilczek and A. Zee, “Families From Spinors,” Phys. Rev. D **25**, 553 (1982); J. Maalampi, J.T. Peltoniemi, and M. Roos, PLB 220, 441(1989); J. Maalampi and M. Roos, “Physics Of Mirror Fermions,” Phys. Rept. **186**, 53 (1990); K. S. Babu, I. Gogoladze, P. Nath and R. M. Syed, “A Unified framework for symmetry breaking in SO(10),” Phys. Rev. D **72**, 095011 (2005) [hep-ph/0506312]; “Fermion mass generation in SO(10) with a unified Higgs sector,” Phys. Rev. D **74**, 075004 (2006), [arXiv:hep-ph/0607244]; “Variety of SO(10) GUTs with Natural Doublet-Triplet Splitting via the Missing Partner Mechanism,” Phys. Rev. D **85**, 075002 (2012) [arXiv:1112.5387 [hep-ph]]; P. Nath and R. M. Syed, “Yukawa Couplings and Quark and Lepton Masses in an SO(10) Model with a Unified Higgs Sector,” Phys. Rev. D **81**, 037701 (2010).
- [3] T. Ibrahim and P. Nath, Phys. Rev. D **84**, 015003 (2011) [arXiv:1104.3851 [hep-ph]].
- [4] T. Ibrahim and P. Nath, Phys. Rev. D **82**, 055001 (2010) [arXiv:1007.0432 [hep-ph]].
- [5] T. Ibrahim and P. Nath, Phys. Rev. D **81**, no. 3, 033007 (2010) [Erratum-ibid. D **89**, no. 11, 119902 (2014)] [arXiv:1001.0231 [hep-ph]].
- [6] T. Ibrahim and P. Nath, Phys. Rev. D **78**, 075013 (2008) [arXiv:0806.3880 [hep-ph]].
- [7] T. Ibrahim and P. Nath, Nucl. Phys. Proc. Suppl. **200-202**, 161 (2010) [arXiv:0910.1303 [hep-ph]].
- [8] T. Ibrahim and P. Nath, Phys. Rev. D **87**, no. 1, 015030 (2013) [arXiv:1211.0622 [hep-ph]].
- [9] T. Ibrahim, A. Itani and P. Nath, Phys. Rev. D **90**, no. 5, 055006 (2014).
- [10] T. Ibrahim, A. Itani and P. Nath, arXiv:1406.0083 [hep-ph].
- [11] A. Aboubrahim, T. Ibrahim and P. Nath, Phys. Rev. D **89**, no. 9, 093016 (2014) [arXiv:1403.6448 [hep-ph]].
- [12] A. Aboubrahim, T. Ibrahim, A. Itani and P. Nath, Phys. Rev. D **89**, no. 5, 055009 (2014) [arXiv:1312.2505 [hep-ph]].
- [13] A. Aboubrahim, T. Ibrahim and P. Nath, Phys. Rev. D **88**, 013019 (2013) [arXiv:1306.2275 [hep-ph]].
- [14] K. S. Babu, I. Gogoladze, M. U. Rehman and Q. Shafi, Phys. Rev. D **78**, 055017 (2008) [arXiv:0807.3055 [hep-ph]].

- [15] C. Liu, Phys. Rev. D **80**, 035004 (2009) [arXiv:0907.3011 [hep-ph]].
- [16] S. P. Martin, Phys. Rev. D **81**, 035004 (2010) [arXiv:0910.2732 [hep-ph]].
- [17] F. Gabbiani and A. Masiero, Nucl. Phys. B **322**, 235 (1989).
- [18] R. L. Arnowitt and P. Nath, Phys. Rev. Lett. **66**, 2708 (1991).
- [19] F. Gabbiani, E. Gabrielli, A. Masiero and L. Silvestrini, Nucl. Phys. B **477**, 321 (1996) [hep-ph/9604387].
- [20] A. Abada, C. Biggio, F. Bonnet, M. B. Gavela and T. Hambye, Phys. Rev. D **78**, 033007 (2008) [arXiv:0803.0481 [hep-ph]].
- [21] W. Altmannshofer, A. J. Buras, S. Gori, P. Paradisi and D. M. Straub, Nucl. Phys. B **830**, 17 (2010) [arXiv:0909.1333 [hep-ph]].
- [22] D. McKeen, M. Pospelov and A. Ritz, Phys. Rev. D **87**, no. 11, 113002 (2013) [arXiv:1303.1172 [hep-ph]].
- [23] J. L. Hewett, H. Weerts, R. Brock, J. N. Butler, B. C. K. Casey, J. Collar, A. de Gouvea and R. Essig *et al.*, arXiv:1205.2671 [hep-ex].
- [24] T. Ibrahim and P. Nath, Rev. Mod. Phys. **80**, 577 (2008) [arXiv:0705.2008 [hep-ph]].
- [25] J. Baron *et al.* [ACME Collaboration], Science **343**, 269 (2014) [arXiv:1310.7534 [physics.atom-ph]].
- [26] B. Aubert *et al.* [BaBar Collaboration], Phys. Rev. Lett. **104**, 021802 (2010) [arXiv:0908.2381 [hep-ex]].
- [27] K. Hayasaka *et al.* [Belle Collaboration], Phys. Lett. B **666**, 16 (2008) [arXiv:0705.0650 [hep-ex]].
- [28] G. Hinshaw *et al.* [WMAP Collaboration], Astrophys. J. Suppl. **208**, 19 (2013) [arXiv:1212.5226 [astro-ph.CO]].
- [29] T. Schwetz, M. A. Tortola and J. W. F. Valle, New J. Phys. **10**, 113011 (2008) [arXiv:0808.2016 [hep-ph]].
- [30] Particle Data Group, Chin. Phys. C, 38, 090001 (2014).
- [31] G. Aad *et al.* [ATLAS Collaboration], JHEP **1405**, 071 (2014) [arXiv:1403.5294 [hep-ex]].
- [32] G. Aad *et al.* [ATLAS Collaboration], JHEP **1404**, 169 (2014) [arXiv:1402.7029 [hep-ex]].